7-1-2004

The distance and interstellar sight line to GX 339-4

R. I. Hynes
The University of Texas at Austin

D. Steeghs
Harvard-Smithsonian Center for Astrophysics

J. Casares
Instituto Astrofisico de Canarias

P. A. Charles
University of Southampton

K. O'Brien
European Southern Observatory Santiago

Recommended Citation

Hynes, R., Steeghs, D., Casares, J., Charles, P., & O'Brien, K. (2004). The distance and interstellar sight line to GX 339-4. *Astrophysical Journal, 609* (1 I), 317-324. https://doi.org/10.1086/421014

The Astrophysical Journal, 609:317–324, 2004 July 1

THE DISTANCE AND INTERSTELLAR SIGHT LINE TO GX 339−4

R. I. Hynes,[1,2] D. Steeghs,[3] J. Casares,[4] P. A. Charles,[5] and K. O'Brien[6]

Received 2004 February 2; accepted 2004 March 15

ABSTRACT

The distance to the black hole binary GX 339−4 remains a topic of debate. We examine high-resolution optical spectra of the Na D lines resolving the velocity structure along the line of sight. We find this to be complex, with at least nine components, mostly blueshifted, spanning a velocity range of nearly 200 km s^{-1}. The presence of components with a large blueshift rules out a nearby location and requires that the binary be located at or beyond the tangent point, implying a lower limit to the distance of ∼6 kpc. The presence of a significant redshifted component at +30 km s^{-1} is even more intriguing, as GX 339−4 also has a slightly positive systemic velocity, suggesting that the source, and this cloud, could be on the far side of the Galaxy, where the radial velocities due to Galactic rotation become positive again. If this is the case, we require a distance of ∼15 kpc. This is less secure than the 6 kpc lower limit, however. We discuss the implications of these possible distances for the outburst and quiescent luminosities, as well as the nature of the companion star, and argue that a large distance explains these characteristics. In particular, it would explain the nondetection of the companion star during the faintest states.

Subject headings: black hole physics — stars: distances — stars: individual (GX 339−4) — X-rays: binaries — X-rays: individual (GX 339−4)

1. INTRODUCTION

The distance of X-ray binaries is challenging to determine precisely. They are usually too distant for current parallax measurements, and there are no really reliable standard candles other than type I X-ray bursts showing radius expansion, and these only occur in a subset of neutron star systems (see Kuulkers et al. 2003 and references therein). For black holes, such as GX 339−4, the problem is much less tractable. Fortunately the majority of such systems undergo periods of deep quiescence when it is possible to detect the companion star and determine the binary parameters. Hence both the radius and temperature (i.e., surface brightness) can be estimated and the distance derived from the apparent brightness (see, e.g., Gelino et al. 2001). For GX 339−4 this is not possible, as even in a very low luminosity state, no spectral features of the companion star were seen in the Very Large Telescope (VLT) FORS observations (Shahbaz et al. 2001). This is frustrating for distance and parameter estimation and is very puzzling in its own right. One explanation for the nondetection of the companion is that the distance has been significantly underestimated.

Current distance estimates are very uncertain; Buxton & Vennes (2003) have provided a convenient summary. Early estimates were rather low, mostly falling in the 1–4 kpc range. More recently, larger estimates have been proposed. The nondetection of the companion star (Shahbaz et al. 2001) was used as evidence for a distance $\gtrsim$5.6 kpc. A more novel approach was taken by Maccarone (2003), who has shown that in most black hole binaries, transitions between the high/soft and low/hard states occur at approximately a fixed fraction of the Eddington limit. It was suggested that the transition luminosity can then be used as a mass-dependent standard candle. Assuming a minimum black hole mass for GX 339−4 of $\gtrsim$5.8 $M_\odot$ (Hynes et al. 2003), Maccarone (2003) estimates a distance $\gtrsim$6 kpc, allowing for scatter about the relation.

The actual distance of GX 339−4 thus remains very uncertain, but could be rather large. This introduces considerable uncertainty into interpreting its quiescent and outburst luminosities and the nature of the companion. The distance also has important implications for interpretation of the recently discovered resolved jets; Gallo et al. (2004) estimated that the motion of the jet head requires an apparent velocity of 0.9c even at 4 kpc. A significantly larger distance would therefore imply apparent superluminal motion. We have therefore analyzed interstellar features in high-resolution spectra described in § 2 to elucidate the properties of the line of sight in more detail. In § 3 we perform a detailed study of the properties of line-of-sight Na I and Ca II absorption, resolving most individual clouds in Na I and hence determining cloud-by-cloud velocities, velocity dispersions, and Na I column densities. We also have some information about the relative abundances of Ca II to Na I as a function of velocity. We discuss the implications for the distance of GX 339−4 in § 4 and for its reddening in § 5. Finally, in § 6 we consider how the range of distances proposed affects estimates of the outburst and quiescent X-ray luminosities and the nature of the companion star, and in § 7 we summarize our conclusions.

2. OBSERVATIONS

High-resolution observations of GX 339−4 were obtained with the UV-Visual Echelle Spectrograph (UVES) on UT2 (Kueyen) at the VLT on 2002 August 9–15. These spanned a

[1] Astronomy Department and McDonald Observatory, University of Texas at Austin, 1 University Station C1400, Austin, TX 78712; rih@astro.as.utexas.edu.
[2] Hubble Fellow.
[3] Harvard-Smithsonian Center for Astrophysics, 60 Garden Street, MS-67, Cambridge, MA 02138; dsteeghs@head-cfa.harvard.edu.
[4] Instituto de Astrofísica de Canarias, 38200 La Laguna, Tenerife, Spain; jcv@ll.iac.es.
[5] School of Physics and Astronomy, University of Southampton, Highfield, Southampton SO17 1BJ, UK; pac@astro.soton.ac.uk.
[6] European Southern Observatory, Casilla 19001, Santiago 19, Chile; kobrien@eso.org.

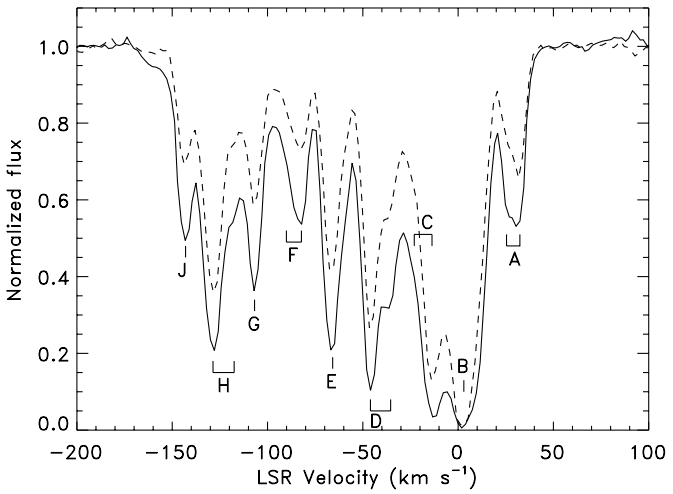

FIG. 1.—Line profiles of the Na D1 (*dashed*) and Na D2 (*solid*) lines. Spectra have been normalized, but no offset is applied between the lines. Labels denote distinct components, with vertical tick marks indicating the components fitted in Table 1. Some of these (e.g., D) appear to be further unresolved multiples.

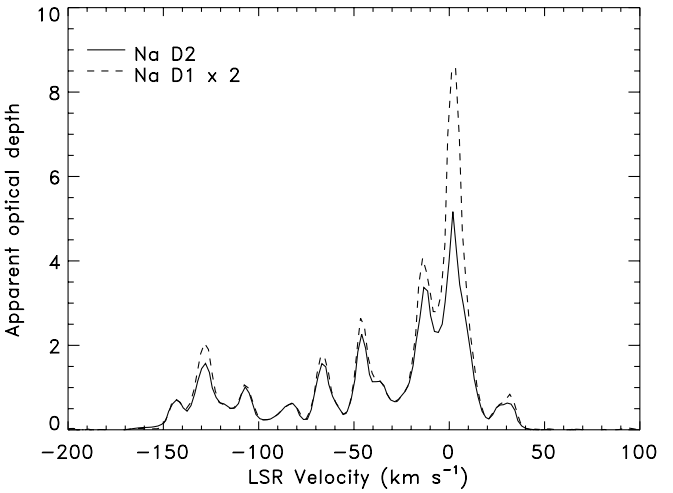

FIG. 2.—Apparent optical depths of the Na D lines. The D1 optical depths have been doubled so that they are identical to D2 in the optically thin limit. Where the lines disagree, saturation is important and the optical depth may be underestimated.

wavelength range of 4100–6200 Å and included a total exposure time of 12 hr, yielding a superb-quality average spectrum (signal-to-noise ratio near the Na D lines greater than 100 without binning). A 1″ slit was used, giving a nominal resolution near the Na D lines of $\simeq$44,000, corresponding to a kinematic resolution of 6.8 km s^{-1}. The starlight is concentrated at the center of the slit, however, yielding a somewhat higher resolution. From the spatial profiles near Na D we estimate a mean seeing of about 0.″5, implying that the resolution could be as good as 4 km s^{-1} with a 1″ slit. In practice, this is not realized, and we expect a value between these extremes. We therefore leave the instrumental resolution as a free parameter in subsequent fits. For the rest of this work we focus only upon the Na D1 and D2 lines (5895.92 and 5889.95 Å, respectively). Pipeline optimal extractions were supplied and were of good quality in this region; a manual reduction of selected spectra yielded negligible improvement.

We supplement these data with lower resolution observations of the Ca II H and K lines (3968.47 and 3933.66 Å, respectively). These were obtained with the Royal Greenwich Observatory spectrograph of the Anglo-Australian Telescope (AAT) over 2002 June 6–11, with the R1200B grating yielding a wavelength coverage of 3500–5250 Å. The images were debiased and flat-fielded and the spectra subsequently extracted using conventional optimal extraction techniques (Horne 1986). Wavelength calibrations were interpolated between CuAr comparison lamp images obtained every 20–30 minutes. The kinematic resolution is estimated to be 74 km s^{-1}.

3. LINE-OF-SIGHT VELOCITY STRUCTURE

3.1. Na I *Absorption*

We show line profiles of the two Na D lines in Figure 1 relative to the local standard of rest (LSR). They are clearly complex with a large velocity dispersion, suggesting a relatively large distance. This immediately rules out suggestions that GX 339−4 is a local object at $\sim$1.3 kpc (Mauche & Gorenstein 1986; Predehl et al. 1991); the same conclusion was drawn by Zdziarski et al. (1998) for different reasons.

We can obtain an approximate estimate of the distribution of Na I with velocity by converting the line profiles into apparent optical depths (Fig. 2), as discussed by Sembach et al. (1993). This is not the true optical depth, because it is modified by instrumental broadening. It is also reduced (relative to the Na I column density) for strongly saturated components. This is seen in differences in the optical depths inferred from the D1 and D2 lines. We have scaled up the D1 optical depths in Figure 2 by a factor of 2 (the ratio of oscillator strengths) so that the two lines can be directly compared. Where the two optical depth profiles overlap (i.e., the D1 line has exactly half the optical depth of the D2 line), the apparent optical depths are simply blurred versions of the true optical depth, and the relative contributions of different components are preserved. Where unresolved saturated structure is present, the D2 line becomes preferentially more saturated, the D1 line becomes proportionately stronger, and the ratio of apparent optical depths approaches unity. In this case the total absorption of a component is underestimated, but the D1 optical depths reflect the column densities more accurately. We can see that most of the absorption column appears to be at low velocities, $|V_{\rm LSR}| \lesssim 20$ km s^{-1}, especially when one considers that these are the most saturated components and hence the most severely underestimated. There is also a significant contribution at higher velocities, however.

We can perform a more quantitative analysis by modeling the line profiles and explicitly accounting for unresolved saturation. We follow standard techniques (e.g., Spitzer 1978; Sembach et al. 1993), as also applied by Dubus et al. (2001) to Ca II lines in XTE J1118+480. We assume that the line-of-sight absorption consists of a number of discrete clouds, each of which has mean velocity v, a Gaussian distribution of velocities with width b, and Na I column density n. Given this model we can simultaneously predict both D1 and D2 intrinsic line profiles. We then convolve these with the instrumental resolution and compare with the data. As discussed above, the exact instrumental resolution is uncertain and was fitted as a free parameter. The best fit was obtained for 6.0 km s^{-1}, which falls within the range expected given the slit width and seeing (§ 2). Note that in most cases these parameters are relatively well constrained, even though the intrinsic widths are not fully resolved. This is because the differential saturation of the D1 and D2 lines makes the ratio of the two line strengths sensitive to the intrinsic widths. Hence, we can recover a reasonable

TABLE 1
RESULTS OF FITS TO THE Na D LINES

Component	v[a] (km s^{-1})	b[b] (km s^{-1})	n[c] (10^{12} cm^{-2})
Single Component B			
A1	$32.4^{+0.6}_{-0.3}$	$1.5^{+0.2}_{-0.5}$	$0.80^{+0.15}_{-0.23}$
A2	$25.4^{+1.2}_{-0.4}$	$2.2^{+2.3}_{-0.5}$	$0.45^{+0.05}_{-0.04}$
B	3.0 ± 0.1	7.3 ± 0.2	$12.7^{+0.7}_{-0.5}$
C1	$-13.7^{+0.2}_{-0.3}$	$2.7^{+0.5}_{-2.7}$	$8.3^{+\infty}_{-2.6}$
C2	$-23.0^{+1.8}_{-1.6}$	$7.4^{+1.9}_{-2.4}$	1.17 ± 0.35
D1	-35.4 ± 0.3	$2.2^{+0.5}_{-0.3}$	$0.94^{+0.10}_{-0.09}$
D2	-46.0 ± 0.1	4.0 ± 0.2	$3.05^{+0.14}_{-0.12}$
E	-65.8 ± 0.1	5.1 ± 0.2	2.04 ± 0.05
F1	$-82.2^{+0.3}_{-0.4}$	$2.1^{+0.6}_{-0.4}$	0.53 ± 0.08
F2	$-90.1^{+1.0}_{-1.2}$	$6.6^{+1.2}_{-1.3}$	$0.45^{+0.07}_{-0.08}$
G	-106.8 ± 0.2	$3.7^{+0.4}_{-0.3}$	1.10 ± 0.04
H1	-117.5 ± 0.4	$1.2^{+0.6}_{-0.4}$	$0.44^{+0.42}_{-0.05}$
H2	-128.6 ± 0.1	4.4 ± 0.3	$2.32^{+0.09}_{-0.08}$
J	-143.0 ± 0.2	$2.7^{+0.4}_{-0.3}$	$0.75^{+0.06}_{-0.04}$
Split Component B[d]			
B1	$12.6^{+0.5}_{-0.7}$	$3.1^{+0.7}_{-0.5}$	$1.06^{+0.21}_{-0.13}$
B2	2.3 ± 0.1	$3.0^{+0.4}_{-0.5}$	250^{+1060}_{-150}
C1[e]	-13.3 ± 0.2	$5.5^{+0.4}_{-0.5}$	$5.20^{+0.16}_{-0.15}$
C2	$-26.4^{+0.6}_{-0.5}$	$3.1^{+1.4}_{-1.1}$	$0.53^{+0.12}_{-0.07}$

[a] Mean velocity.
[b] Gaussian width.
[c] Na I column density.
[d] Revised parameters for B and C. Other components are unaffected.
[e] There is no formal lower limit on the width of component C1 or a corresponding upper limit on the column density.

estimate of the column density even for somewhat saturated lines. The largest uncertainty exists where significant saturation is present, and then we sometimes only constrain a lower limit upon the column density. Fitting was performed iteratively using the Levenberg-Marquardt algorithm (see, e.g., Press et al. 1992). We began by fitting the components labeled in Figure 1. Additional components were added when it was clear that they were needed; for example, D clearly includes an additional low-velocity component, and a weak component is also needed between G and H. Other deficiencies were apparent only by comparison with the preliminary fits and led us to add additional components near C and F as well. It may be that such weak components from small clouds are actually present throughout the profile but are only discernible in the gaps between the larger components (S. Redfield 2004, private communication).

The derived parameters for the components are listed in Table 1. This model reproduced the data extremely well, with no significant residuals, so we have not shown the fit. Velocities are derived from both D1 and D2 lines simultaneously and indicate a range of mean cloud velocities of -143 to $+32$ km s^{-1}. We compare this to Galactic rotation curves in § 4. Component widths are 1.2–7.4 km s^{-1}. These values are typical of the interstellar medium (ISM); Sembach & Danks (1994) found average values for the Na D lines of 4.0 km s^{-1}. If the lowest widths are purely thermal, they indicate cloud temperatures of $\gtrsim$3000 K, but turbulent broadening could be present as well. It may be that some of the larger widths, such as that of component B, indicate additional unresolved components rather than intrinsically high widths. One of these mechanisms is needed for the highest widths, as these are too high for thermal broadening alone. We derive a total Na I column density of at least 3.5×10^{13} cm^{-2}, of which components B and C (assumed to be relatively local) contribute at least 63%.

In most cases the sensitivity to unresolved blends is weak, as the components are not strongly saturated and the total column density is approximately conserved. For component B, however, the total column density is sensitive to assumed substructure. To illustrate this, we repeated the fitting with two subcomponents; the results are shown in Table 1. This allows the main component to be narrower and hence saturate more easily. A much larger column density is then required to achieve the same equivalent width of absorption. Consequently, the single-component fit should be considered the lower limit on the column density in the B–C complex (2.2×10^{13} cm^{-2}). This implies that the total column density estimated above and the fraction of total column contained within the B–C complex are also lower limits. Similar difficulties exist for components C1 and H1, and large column densities cannot be formally rejected in either case. This reflects the significant saturation also present in these components (Fig. 2).

3.2. Ca II *Absorption*

The resolution of the AAT observations of the Ca II lines is not sufficient to perform a similar component-by-component analysis. We can, however, use the model derived from the Na D lines to predict the lower resolution profiles and perform a crude comparison. To do this we initially assume a ratio of Ca II to Na I column densities of 0.6, appropriate for inner Galactic center sight lines (Sembach & Danks 1994), and an

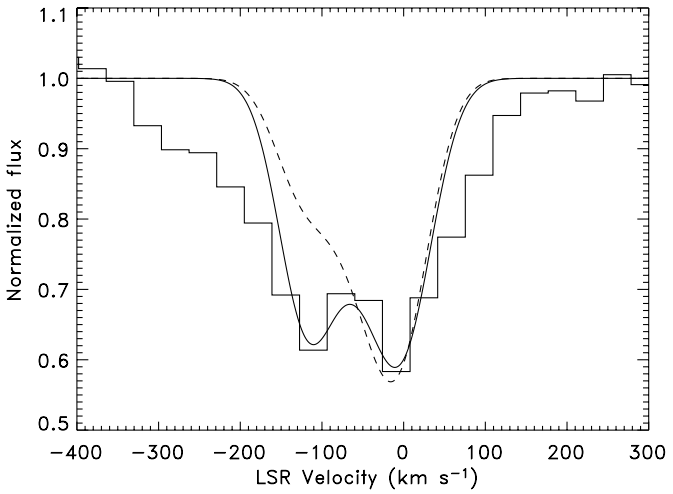

FIG. 3.—Line profile of the Ca II K line. Histograms show the data, which are at much lower resolution than that of the Na D lines. The dashed line shows a "blind" prediction of the line profile based on the Na D fits, assuming that no velocity correction is needed, that the intrinsic component widths are thermal, and that the ratio of Ca II to Na I is 0.6, appropriate for inner Galactic center lines of sight (Sembach & Danks 1994). The solid line is a better fit, including a small velocity offset and allowing the abundance of the G–J complex to differ from the rest of the components. See the text for more details.

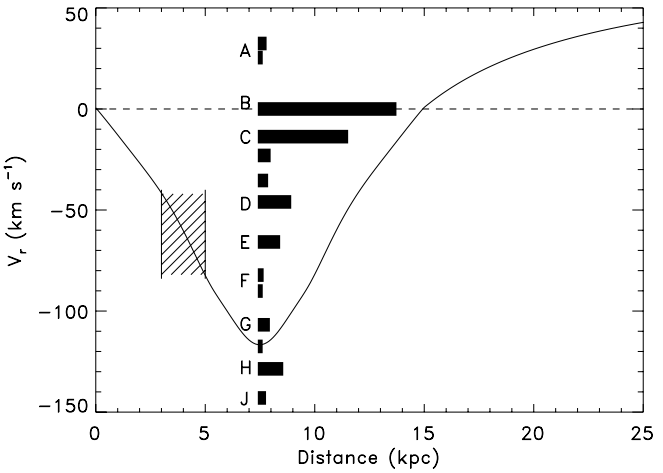

FIG. 4.—Expected relation between radial velocity and distance along the line of sight to GX 339−4. The curve uses the rotation curve adopted by Nakanishi & Sofue (2003). Each horizontal bar represents one of the fitted components of Na D absorption. The vertical position indicates the fitted velocity, and the length of the bar is proportional to the column density. The horizontal positions are arbitrary. The hatched region indicates the distance range favored by Zdziarski et al. (1998).

instrumental resolution of 74 km s^{-1}. The intrinsic width of each component is scaled down by 0.76, which is appropriate if it is dominated by thermal broadening (i.e., scaling by the square root of the atomic weight). The fit to the profile of the K line is shown in Figure 3; the H line is not used because it is blended with Balmer emission, but the line profile otherwise appears to be similar. The abundance ratio assumed clearly underestimates the Ca II absorption at higher velocities. To improve the fit, we recalculated assuming a small velocity offset (5 km s^{-1}; a small fraction of a resolution element) for the AAT spectra and a slightly lower ratio of Ca II to Na I of 0.53 for most components, but a higher ratio of 4.5 for components G–J. If we alternatively keep the intrinsic width, b, fixed (appropriate for turbulent broadening), then we require abundance ratios of 0.42 and 2.5 for low- and high-velocity components, respectively. Either model provides a much better fit, although it clearly still underestimates the wings of the Ca II profiles. This is a common feature; additional Ca II absorption is often seen at high velocities (beyond those allowed by Galactic rotation) where Na I absorption is weak or absent (Sembach & Danks 1994). It has been attributed to a significantly enhanced abundance of gas-phase calcium (by a factor of 50 or more relative to sodium) in the high-velocity components of the ISM via collisional destruction of dust grains. It is also observed that the mean calcium abundance is enhanced along halo sight lines (Sembach & Danks 1994), although this may simply reflect the preponderance of high-velocity material at high latitudes. Other than such diagnostics, the Na I lines are more useful, as they are more closely related to Galactic rotation and correlate better with $E(B-V)$.

4. THE DISTANCE TO GX 339−4

We have mapped out the properties of gas clouds along the line of sight to GX 339−4 in velocity space. We now attempt to associate these with distance, assuming the velocity is due to Galactic rotation, and hence derive a lower limit on the distance to GX 339−4. Qualitatively we expect to see low-velocity material from the solar neighborhood and increasingly negative velocities as the tangent point is approached. Beyond this, velocities become less negative again and become positive at distances outside the solar circle. The preponderance of absorption components with negative velocities is thus as expected from Galactic rotation along this sight line. To be more quantitative, we show the expected velocity as a function of distance in Figure 4. We assumed the rotation curve prescription of Clemens (1985), with the modified polynomial coefficients of Nakanishi & Sofue (2003). These were derived for a solar Galactocentric radius of $R_0 = 8.0$ kpc and velocity of $\Theta_0 = 217$ km s^{-1}, consistent with the most recent geometric determination of the distance to the Galactic center ($R_0 = 7.94 \pm 0.42$ kpc, $\Theta_0 = 220.7 \pm 12.7$ km s^{-1}; Eisenhauer et al. 2003). Figure 4 also indicates the velocity and relative column density of each fitted absorption component for easy comparison with the predicted velocities.

Components B and C in GX 339−4 likely correspond to local material and contribute $\gtrsim$63% of the total Na I column density. The velocities correspond to a distance $\lesssim$2 kpc, but the material could be within 1 kpc, allowing for a 10 km s^{-1} dispersion in mean velocities. For a Galactic latitude of $-4.^{\circ}5$, this material will thus be $\lesssim$0.16 kpc below the plane and well within the Na I layer (which has an estimated scale height of $0.43^{+0.12}_{-0.08}$ kpc; Sembach & Danks 1994). Examination of field stars near GX 339−4, at distances up to 2 kpc, suggests that local material within this distance accounts for $\sim 2/3$ of the reddening to GX 339−4, consistent with this (Zdziarski et al. 1998).

If the distance to GX 339−4 were $\sim$4 kpc, as proposed by Zdziarski et al. (1998) and Buxton & Vennes (2003), then the maximum expected negative velocity would be ~ -60 km s^{-1}. Components D and E could be corotating, but the G–J complex would require peculiar velocities of 40–80 km s^{-1}. The latter accounts for $\lesssim$13% of the total column density, and as we have already noted is relatively overabundant in Ca II. There are two possible interpretations for this high-velocity absorption. We consider the most likely to be that it is corotating with the Galactic rotation curve. In support of this, the similarity of the velocities of the G–J complex to the predicted

tangent-point velocity of approximately −120 km s^{-1} is suggestive. The range of velocities is also in very good agreement with CO maps, which exhibit a vertically integrated range of velocities to −140 km s^{-1} for this Galactic longitude (Dame et al. 2001). The inferred altitude of the tangent-point material is ∼0.55 kpc. This is not a serious problem given a scale height of 0.43 kpc. The alternative explanation is that the G–J complex (and component F) arises from closer material with large peculiar velocities; this would be the same material as the "forbidden velocity" gas of Sembach & Danks (1994). The enhanced Ca II abundance would be typical of such gas. We believe that the presence of multiple components contributing a significant fraction of the Na I column at such high velocities is very unlikely, however. Such features are not seen in Na I in any of the similar lines of sight collected by Sembach et al. (1993), and Sembach & Danks (1994) estimated that even the velocity dispersion of the *high-velocity* Ca II absorption components was only 21.3 km s^{-1}. If GX 339−4 lies at 4 kpc, it would therefore have a rather unusual line of sight. Neither are such extreme velocities seen in any of the spectra of local stars presented by Welty & Hobbs (2001). Consequently, it seems more likely that most of the absorption velocities do indicate Galactic rotation and that GX 339−4 lies at or beyond the tangent point. The implied distance is then ≳6 kpc, allowing for some uncertainty in rotation curves and the intrinsic velocity dispersion of the absorbing clouds.

Beyond this, the situation is less clear. This is because the velocities increase again, and so there is ambiguity between close and distant material. Components D–F could arise on either side of the tangent point, and it is hard to make a conclusive statement about how far beyond this GX 339−4 could lie. Two lines of argument suggest that a significantly larger distance is possible, but neither are conclusive. One is the systemic velocity of GX 339−4 itself. The best estimate of this comes from the emission-line radial velocity analysis of the same data set used here (Hynes et al. 2003), with He II emission-line wings suggesting $\gamma = +12.3 \pm 1.0$ km s^{-1} and Bowen lines consistent with this for the preferred orbital period. This would of course be expected for a local object, but the Na D velocity dispersion rules this out, even if earlier arguments do not. If GX 339−4 lies at the tangent point, however, then the peculiar radial velocity would be ∼+140 km s^{-1}. This is unusually large for a black hole binary, as White & van Paradijs (1996) estimated that their radial velocity dispersion should be 40 km s^{-1} based on their distances from the plane and consistent with measurements. Larger values are not impossible (e.g., GRO J1655−40 has an estimated peculiar radial velocity of 114 km s^{-1}; Brandt et al. 1995) but are thought to arise when black holes are formed by fallback onto a neutron star that received a kick (Fryer & Kalogera 2001). A large velocity is only expected for a low-mass black hole, however, which is inconsistent with the high mass function of GX 339−4 and the lack of evidence for a high inclination. Further increasing the distance is therefore appealing, as it would reduce this required peculiar velocity. A location close to the solar circle on the far side of the Galaxy (≳15 kpc) would require negligible peculiar velocity, consistent with most Galactic black hole binaries. The other argument comes from the one absorption feature we have not yet accounted for: component A. This has two subcomponents with *positive* velocity, 25–35 km s^{-1}. If this arises locally, then it arises from material with a forbidden velocity ≳25 km s^{-1}. Given that there are only two weak components (or one with a complex profile) and that the total contribution to the column density is ≲4%, this is not impossible. This material could also arise on the far side of the Galaxy, and it would then have a radial velocity close to that of the source. One could argue that since GX 339−4 has a Galactic latitude of −4.°5, at this distance, the line of sight should be more than 1 kpc below the plane. However, the Galaxy does exhibit warps, and the outer disk warps downward toward the line of sight of GX 339−4 (Nakanishi & Sofue 2003). It is possible that GX 339−4 and the redshifted absorption are associated with this warped material.

We thus conclude that a minimum distance of 6 kpc is required, based on the presence of intervening material with large blueshifts, consistent with expected tangent-point velocities. The presence of redshifted absorption, together with the low systemic velocity of GX 339−4 itself, suggests that a much larger distance ≳15 kpc might be correct, although a large peculiar velocity for GX 339−4 together with forbidden velocity gas could obviate this. GX 339−4 is thus farther away than most previous estimates (but see Shahbaz et al. 2001 and Maccarone 2003) and possibly a lot farther.

5. THE REDDENING OF GX 339−4

Our high-quality spectra should also allow us to obtain more robust reddening constraints from the Na D lines; we do not attempt this with the Ca II lines, as these do not trace the dust as well (Sembach & Danks 1994).

The integrated Na D equivalent width (EW) has been estimated by a number of authors. The most recent values are 3.7 Å (Soria et al. 1999) and 4.2 ± 1.0 Å (Buxton & Vennes 2003). We estimate a total EW of 3.57 ± 0.02 Å from our resolved Na D lines, with 1.48 ± 0.01 Å and 2.10 ± 0.01 Å in the Na D1 and D2 lines, respectively, consistent with other estimates. The uncertainties quoted are conservative estimates based on the range of possible continuum levels; formal statistical errors are smaller than this. The interpretation of the equivalent width is obviously complicated by saturation of some components, but neglecting this, we recover a lower limit of $E(B-V) \gtrsim 0.6$ from the Na D2 line, assuming the asymptotic linear calibration of Munari & Zwitter (1997). We can perform an analogous calculation using the less saturated Na D1 line, since in the optically thin limit the D2/D1 ratio has a value of 2. This yields a lower limit of $E(B-V) \gtrsim 0.85$.

An alternative approach is to circumvent the saturation effects by using the column density derived from the line profile fits. As with all such calibrations, it is still sensitive to assumptions about gas-to-dust scaling ratios. We use the values derived by Sembach & Danks (1994), which include scalings for a number of types of sight line. An Na I column of at least 3.5×10^{13} cm^{-2} corresponds to $N_{\rm H} = 3.1 \times 10^{21}$ cm^{-2} and $E(B-V) = 0.50$ using ratios appropriate to inner Galactic center sight lines. These values change to $N_{\rm H} = 3.3 \times 10^{21}$ cm^{-2} and $E(B-V) = 0.69$ using Galactic center ratios and $N_{\rm H} = 4.4 \times 10^{21}$ cm^{-2} and $E(B-V) = 0.59$ for averaged ratios. The uncertainty is larger than implied by the scatter between these estimates, however, since the variance in ratios within each of these samples is large. While some of the variance may simply reflect measurement errors, it is likely that the ratios are subject to significant cloud-to-cloud scatter. As discussed earlier, these are also lower limits, since the local components of Na D are saturated and the column density used here may have been significantly underestimated. This is likely why both the $N_{\rm H}$ and $E(B-V)$ values we estimate are lower than other measurements (e.g., Zdziarski et al. 1998; Corongiu et al. 2003; Miller et al. 2004).

Consequently, even with the detailed resolution presented here, we cannot determine a reliable $E(B-V)$ from the Na D lines; this method is fundamentally rather crude and limited by saturation. All we can say with confidence is that the reddening is greater than 0.5 and probably greater than about 0.8. This is comparable to previous estimates, including 1.2 ± 0.1 (Zdziarski et al. 1998) and 1.1 ± 0.2 (Buxton & Vennes 2003). We suspect that these quoted uncertainties are underestimates, however, as similar difficulties apply as with our own measurements; indeed, the latter estimate is also based on Na D. Upper limits are problematic, and neither the methods of Zdziarski et al. (1998) nor Buxton & Vennes (2003) nor our discussion above adequately address this. Neutral hydrogen column densities do allow a crude upper limit, however. A range of values are derived (see references above), but all imply $N_{\rm H} \lesssim 7 \times 10^{21}$ cm^{-2}. Similarly, a range of gas-to-dust scalings exist, but that of Bohlin et al. (1978), with an assumed 30% uncertainty, encompasses all of them and also accounts for the variance between lines of sight. Using this scaling and the upper limit on $N_{\rm H}$ implies $E(B-V) \lesssim 1.6$. The actual value could well be much less than this. An independent check is provided by the Galactic dust maps of Schlegel et al. (1998), which imply $E(B-V) \sim 0.9$, although their use for Galactic latitudes less than 5° is not recommended by the authors.

6. DISCUSSION

6.1. *The Outburst Luminosity*

The luminosity of the transition between high/soft and low/hard states in black holes is of interest (Maccarone 2003), and it may even be an approximate standard candle. As already noted, Maccarone (2003) estimated a minimum distance of 6 kpc assuming that the minimum black hole mass is given by the mass function of $5.8 \pm 0.5\ M_\odot$ (Hynes et al. 2003). The true mass is likely to be significantly larger than this, however, as the mass function is only approached for high inclinations, and there is no evidence that GX 339−4 has a high inclination; indeed, it has been argued that the inclination is very low (Wu et al. 2001). For actual black hole masses of 10, 15, or 20 $M_\odot$, distances of about 10, 12, or 14 kpc, respectively, would be expected based on the method of Maccarone (2003). These are very reasonable if GX 339−4 lies somewhat beyond the tangent point as we have argued. If it is really beyond 15 kpc, however, then either the black hole mass is relatively high or the transition luminosity is rather high (but not implausibly so).

Zdziarski et al. (1998) have instead tried to use the maximum observed luminosity as a constraint on the distance. We can reverse the argument, however, and examine the maximum luminosity for different possible distances. At 6 kpc, their quoted maximum observed luminosity corresponds to just 10% of the Eddington limit of a 10 $M_\odot$ black hole. This seems rather low, and a higher black hole mass would further exacerbate this. In contrast, for a distance of 15 kpc and black hole masses of 10–20 $M_\odot$, the Eddington ratio is 0.3–0.6, which seems much more in line with other Galactic black hole X-ray binaries. More recent observations provide more stringent constraints, yielding an 0.1–200 keV flux of 5.4×10^{-8} ergs cm^{-2} s^{-1} (extrapolated from a 3–100 keV fit; J. Homan et al. 2004, in preparation). For a 10 $M_\odot$ black hole at distances of 6 and 15 kpc, this corresponds to 20% or 110% of the Eddington limit, respectively. The latter could readily be reconciled with a black hole somewhat more massive than 10 $M_\odot$. Thus, the luminosity is consistent with a relatively large distance given the implied high mass for the black hole.

6.2. *The Quiescent Luminosity*

The X-ray luminosity in the lowest observed state (Gallo et al. 2003) corresponds to 2×10^{33} or 1×10^{34} ergs s^{-1} for distances of 6 or 15 kpc, respectively. Most quiescent black holes have luminosities of between 2×10^{30} and 6×10^{31} ergs s^{-1} (Garcia et al. 2001; Sutaria et al. 2002; Hameury et al. 2003; Tomsick et al. 2003; McClintock et al. 2003). The exception is V404 Cyg (5×10^{33} ergs s^{-1}; Garcia et al. 2001). This is a long-period object (6.5 days) and may be something of an anomaly among quiescent black holes; indeed, it exhibits dramatic X-ray variability (Wagner et al. 1994; Kong et al. 2002; R. Hynes et al. 2004, in preparation), which suggests that it may not be in a fully quiescent state. GX 339−4 appears to have a comparable or larger luminosity at minimum light, so its lowest observed state may also not correspond to the typical quiescent states of transient black hole binaries.

6.3. *The Nature of the Companion Star*

A relatively active system is appealing in light of the nondetection of spectral features from the companion star (Shahbaz et al. 2001). Two explanations exist for this: either the accretion flow is so luminous that it masks the companion star, or the companion is an early-type star with no spectral features in the region studied by Shahbaz et al. (2001). As noted above, a relatively active accretion flow already favors a larger distance, and even 15 kpc gives a plausible luminosity. If we require an early-type companion, then its luminosity will be larger than that of the typical K or M companions of Galactic black holes, and so a large distance might also required to avoid it being visible.

With no detection of the photospheric lines of the companion, its nature is poorly constrained. The companion star should be somewhat evolved, as a 1.7 day orbital period (Hynes et al. 2003) implies a mean density for the companion of only 0.06 g cm^{-3}. This is a factor of 10 below that obtained by Shahbaz et al. (2001), who assumed a shorter orbital period. Such a low density is reached on the main sequence only for B0 stars; it is unlikely that the companion is such a star, however, as it would then be expected to dominate the total light at low luminosities and also significantly affect the motion of the black hole. Hence, the companion of GX 339−4 has a lower density than a main-sequence star of the same temperature. It is probably a subgiant, as late-type giants have even lower densities than we derive for GX 339−4.

For relatively early types, the companion mass is also significant and should result in measurable orbital motion of the accretion disk. Hynes et al. (2003) found no such evidence (only a weak modulation was present, with the wrong phase-dependence) and suggested a mass ratio of $q \lesssim 0.08$. This argues for a companion mass of 1.6 $M_\odot$ or less unless the black hole mass is significantly larger than in other objects ($\gtrsim$20 $M_\odot$), and hence a spectral type of F or later unless the companion is hotter than a main-sequence star of the same mass. In support of these arguments, GRO J1655−40 has a comparable orbital period (2.6 days) and an F companion (Orosz & Bailyn 1997; Shahbaz et al. 1999). Its mass ratio is 0.42 ± 0.03 (Shahbaz 2003); however, the disk lines move with an amplitude of 76.2 ± 7.5 km s^{-1} (Soria et al. 1998),

and the companion totally dominates the optical light in quiescence and remains visible even during outburst. These properties are very different from GX 339−4, which evidently has a much less influential companion. G or K subgiants therefore seem more likely than earlier types.

At our proposed distances there is little difficulty in accommodating such companions. We consider a number of examples. For each we adopt the main-sequence mass corresponding to the spectral type but adjust the radius to fill the Roche lobe. The size of the lobe is constrained by the 1.7 day orbital period, an assumed black hole mass between 5.8 and 20 $M_\odot$, and a mass ratio less than 0.1. The reddening is assumed to be between 0.8 and 1.6, as discussed above. The upper limit is more pertinent, as it makes it easier to hide luminous companions. An F0 star (adopted mass 1.6 $M_\odot$) could only be accommodated if the black hole mass were near 20 $M_\odot$; otherwise, we would expect detectable motion of the accretion disk. At 6 kpc such a star should have an R magnitude of 17.0–19.5, dependent on reddening. This is brighter than the observed faintest magnitude ($R = 20.1$; Shahbaz et al. 2001), so it is unlikely unless the companion is significantly less massive (and hence has a smaller Roche lobe). At 15 kpc, however, this could be as faint as $R = 21.5$, so it could be masked by the accretion light. For a G0 star (assuming $M = 1.1\ M_\odot$), we expect a range of 18.1–20.6 at 6 kpc, or 20.1–22.6 at 15 kpc, and either distance is acceptable, provided the reddening is relatively large. A K0 star ($M = 0.8\ M_\odot$) yields $R = 19.1$–22.7 at 6 kpc and 21.1–24.7 at 15 kpc and poses no difficulties.

These estimates are rather crude and dependent on some assumptions but are probably still useful as approximations. To summarize, the companion to GX 339−4 is likely to be a subgiant, of spectral type G or later if close (∼6 kpc), or possibly F if the distance is much larger.

7. CONCLUSIONS

We have analyzed Na I and Ca II absorption along the line of sight to GX 339−4. We find a rich absorption spectrum with a large velocity dispersion. Velocities are predominantly blueshifted and span the range of velocities expected for Galactic rotation along this line of sight. The presence of multiple features with a significant column density near the tangent-point velocity suggests that GX 339−4 is either at or beyond the tangent point, i.e., $d \gtrsim 6$ kpc. The presence of absorption at redshifted velocities, together with the systemic velocity of GX 339−4 itself, suggest the possibility that the object could be at an even greater distance, on the far side of the Galaxy, $d \gtrsim 15$ kpc. Neither of these pieces of evidence are as secure as that for a location beyond the tangent point, however.

Our analysis also indicates a total Na I column density along the line of sight of at least 3.5×10^{13} cm^{-2}, and this suggests a reddening of at least $E(B-V) = 0.5$, depending on assumed ratios of Na I to dust densities. This is consistent with more straightforward calibrations of the equivalent widths, which imply $E(B-V) \gtrsim 0.85$, but it could be considerably larger dependent on the degree of saturation. Hence, even with well-resolved observations of the Na D lines, it is impossible to derive a precise reddening from these lines, and published estimates should be viewed with caution.

We have examined the implied outburst and quiescent luminosities, and the nature of the companion, in the context of these proposed scenarios. Neither a distance of 6 kpc nor of 15 kpc presents difficulties in these respects. In fact, the larger distance simplifies matters somewhat, for example, in explaining the nondetection of the companion (likely a late-type subgiant) in quiescence. Consequently we propose that a large distance, ∼15 kpc, should be given consideration.

We are grateful to Jeroen Homan, Jon Miller, and Seth Redfield for productive discussions on this topic and to Tom Maccarone for helpful comments on the manuscript. R. I. H. is supported by NASA through Hubble Fellowship grant HF-01150.01-A awarded by STScI. D. S. acknowledges a Smithsonian Astrophysical Observatory Clay Fellowship. J. C. acknowledges support from the Spanish Ministry of Science and Technology through the project AYA2002-03570. This work uses observations collected at ESO in Chile and the Anglo-Australian Telescope. We would particularly like to thank the ESO Director's Office and VLT staff for a generous and efficiently executed award of Director's Discretionary Time. This work has also made use of the NASA ADS Abstract Service, and we are grateful to Craig Markwardt for making the MPFIT IDL fitting routines publicly available.

REFERENCES

Bohlin, R. C., Savage, B. D., & Drake, J. F. 1978, ApJ, 224, 132
Brandt, W. N., Podsiadlowski, P., & Sigurdsson, S. 1995, MNRAS, 277, L35
Buxton, M., & Vennes, S. 2003, MNRAS, 342, 105
Clemens, D. P. 1985, ApJ, 295, 422
Corongiu, A., Chiappetti, L., Haardt, F., Treves, A., Colpi, M., & Belloni, T. 2003, A&A, 408, 347
Dame, T. M., Hartmann, D., & Thaddeus, P. 2001, ApJ, 547, 792
Dubus, G., Kim, R. S. J., Menou, K., Szkody, P., & Bowen, D. V. 2001, ApJ, 553, 307
Eisenhauer, F., Schödel, R., Genzel, R., Ott, T., Tecza, M., Abuter, R., Eckart, A., & Alexander, T. 2003, ApJ, 597, L121
Fryer, C. L., & Kalogera, V. 2001, ApJ, 554, 548
Gallo, E., Corbel, S., Fender, R. P., Maccarone, T. J., & Tzioumis, A. K. 2004, MNRAS, 347, L52
Gallo, E., Fender, R., & Corbel, S. 2003, Astron. Telegram, 196, 1
Garcia, M. R., McClintock, J. E., Narayan, R., Callanan, P., Barret, D., & Murray, S. S. 2001, ApJ, 553, L47
Gelino, D. M., Harrison, T. E., & Orosz, J. A. 2001, AJ, 122, 2668
Hameury, J.-M., Barret, D., Lasota, J.-P., McClintock, J. E., Menou, K., Motch, C., Olive, J.-F., & Webb, N. 2003, A&A, 399, 631
Horne, K. 1986, PASP, 98, 609
Hynes, R. I., Steeghs, D., Casares, J., Charles, P. A., & O'Brien, K. 2003, ApJ, 583, L95
Kong, A. K. H., McClintock, J. E., Garcia, M. R., Murray, S. S., & Barret, D. 2002, ApJ, 570, 277
Kuulkers, E., den Hartog, P. R., in 't Zand, J. J. M., Verbunt, F. W. M., Harris, W. E., & Cocchi, M. 2003, A&A, 399, 663
Maccarone, T. J. 2003, A&A, 409, 697
Mauche, C. W., & Gorenstein, P. 1986, ApJ, 302, 371
McClintock, J. E., Narayan, R., Garcia, M. R., Orosz, J. A., Remillard, R. A., & Murray, S. S. 2003, ApJ, 593, 435
Miller, J. M., et al. 2004, ApJ, 601, 450
Munari, U., & Zwitter, T. 1997, A&A, 318, 269
Nakanishi, H., & Sofue, Y. 2003, PASJ, 55, 191
Orosz, J. A., & Bailyn, C. D. 1997, ApJ, 477, 876
Predehl, P., Braeuninger, H., Burkert, W., & Schmitt, J. H. M. M. 1991, A&A, 246, L40
Press, W. H., Teukolsky, S. A., Vetterling, W. T., & Flannery, B. P. 1992, Numerical Recipes in C (2nd ed.; Cambridge: Cambridge Univ. Press)
Schlegel, D. J., Finkbeiner, D. P., & Davis, M. 1998, ApJ, 500, 525
Sembach, K. R., & Danks, A. C. 1994, A&A, 289, 539
Sembach, K. R., Danks, A. C., & Savage, B. D. 1993, A&AS, 100, 107
Shahbaz, T. 2003, MNRAS, 339, 1031
Shahbaz, T., Fender, R., & Charles, P. A. 2001, A&A, 376, L17
Shahbaz, T., van der Hooft, F., Casares, J., Charles, P. A., & van Paradijs, J. 1999, MNRAS, 306, 89

Soria, R., Wickramasinghe, D. T., Hunstead, R. W., & Wu, K. 1998, ApJ, 495, L95
Soria, R., Wu, K., & Johnston, H. M. 1999, MNRAS, 310, 71
Spitzer, L. 1978, Physical Processes in the Interstellar Medium (New York: Wiley)
Sutaria, F. K., et al. 2002, A&A, 391, 993
Tomsick, J. A., et al. 2003, ApJ, 597, L133
Wagner, R. M., Starrfield, S. G., Hjellming, R. M., Howell, S. B., & Kreidl, T. J. 1994, ApJ, 429, L25
Welty, D. E., & Hobbs, L. M. 2001, ApJS, 133, 345
White, N. E., & van Paradijs, J. 1996, ApJ, 473, L25
Wu, K., Soria, R., Hunstead, R. W., & Johnston, H. M. 2001, MNRAS, 320, 177
Zdziarski, A. A., Poutanen, J., Mikolajewska, J., Gierlinski, M., Ebisawa, K., & Johnson, W. N. 1998, MNRAS, 301, 435